

Hybrid Perovskite Solar Cells: Effects of Conditions in Two-step Fabrication on Obtained Morphology and Power Conversion Efficiency

Apatsanan Phaometvarithorn^{1,2}, Surawut Chuangchote^{3,4,*}, Methawee Nukunudompanich⁵, Manabu Ihara⁵ and Jatuphorn Wootthikanokkhan⁶

¹The Joint Graduate School of Energy and Environment, King Mongkut's University of Technology Thonburi (KMUTT), 126 Prachauthit Rd., Bangmod, Thungkru, Bangkok 10140, Thailand.

²Center of Excellence on Energy Technology and Environment, Ministry of Education, Thailand.

³Department of Tool and Materials Engineering, King Mongkut's University of Technology Thonburi (KMUTT), 126 Prachauthit Rd., Bangmod, Thungkru, Bangkok 10140, Thailand.

⁴Nanoscience and Nanotechnology Graduate Program, King Mongkut's University of Technology Thonburi (KMUTT), 126 Prachauthit Rd., Bangmod, Thungkru, Bangkok 10140, Thailand.

⁵School of Materials and Chemical Technology, Department of Chemical Science and Engineering, Tokyo Institute of Technology, Meguro, Ookayama, 2 Chome 1-2-1, Tokyo 152-8550, Japan.

⁶School of Energy, Environment and Materials, King Mongkut's University of Technology Thonburi (KMUTT), 126 Prachauthit Rd., Bangmod, Thungkru, Bangkok 10140, Thailand.

*Corresponding Author: Surawut Chuangchote, E-mail: surawut.chu@kmutt.ac.th

Abstract: Perovskite solar cells have currently attracted attention in photovoltaic research, because of their promising ways to carry out high performance. The photovoltaic performance of inverted perovskite solar cells with two-step deposition fabrication is strongly influenced by the morphology of perovskite. In this research work, we studied that the effects of optimum conditions (*i.e.* (1) methylammonium iodide (MAI) concentration, (2) MAI dipping duration time, and (3) perovskite annealing time) on obtained morphology and photovoltaic performance in inverted perovskite solar cells with a compact TiO₂ layer (fabricated by spray pyrolysis). The results showed that the optimized morphologies and performances can be obtained from 0.05 M MAI concentration, 5 min MAI dipping duration time, and 90 min perovskite annealing time.

Keywords: Perovskite solar cell; Inverted structure; Morphology; Photovoltaic performance.

1. Introduction

Solar energy is a choice of renewable energies by converting sunlight into electricity through solar photovoltaic (PV) cells or solar cells. Since they can directly convert sun radiation into electricity, the impact to the environment is minimize. Currently, the commercial crystalline silicon solar cells have shown power conversion efficiency (PCE) up to 25%, but these cells are still complicated for production [1]. Therefore, the newest alternative solar cell is hybrid photovoltaic cells, which have attracted many great attentions from researches due to its high PCE and low-cost fabrication [2].

The hybrid solar cells are combinations of organic (conjugated polymer) and inorganic semiconducting materials. They collectively carry the advantages of both materials, such as a direct path for charge transport for increased efficiency, low temperature production to scalability, and lightweight [2-4].

Recently, perovskite solar cells have been attracted considerable interest because of their great promises for development of low-cost thin-film solar cells. They can be reached to 19.3% in 2014, which was achieved within only a few years from the first report in 2009 [5]. The perovskite material structure is ABX₃, which A is a cation (metal or hydrocarbon), B is a metal cation, and X is a halide atom, e.g. CH₃NH₃PbI₃ and CH₃NH₃PbI_{3-x}Cl_x. The hybrid perovskite material exposes small exciton binding energies, suitable direct band gaps, high absorption coefficients, long diffusion lengths, high carrier mobilities, and superior defect tolerances [1,6].

For simple fabrication of perovskite layer, there are many techniques, such as vapor assisted solution process [7], one-step deposition [8-9], and two-step sequential deposition [10-11]. The

morphology and optoelectronic properties were found to be better controlled by two-step deposition method. This method also provided an efficient high performance perovskite solar cells with low-cost process and showed a little *I-V* hysteresis [12]. The most important step of this method is the transformation process from PbI₂ to CH₃NH₃PbI₃, which considerably affected perovskite morphology and photovoltaic performance [13]. Recently, there are many works studied on perovskite morphologies with efficient performances. Im et al. [14] studied effects of CH₃NH₃I (MAI) concentration and Zhao et al. [15] investigated effects of MAI dipping duration time on perovskite performances in inverted perovskite devices with mesoporous TiO₂. Moreover, Barnett et al. [16] investigated effects of perovskite annealing time on photovoltaic performance of ITO/PEDOT:PSS/MAPbI₃/PCBM/C₆₀/BCP/Al. To our knowledge, the literature still does not report the effects of conditions in perovskite fabrication step on obtained morphologies and performances in inverted perovskite solar cells.

In this study, we investigated effects of MAI concentration, MAI dipping duration time, and perovskite annealing time in two-step fabrication on obtained morphology and power conversion efficiency in inverted perovskite solar cells with a compact TiO₂ layer (fabricated by spray pyrolysis).

2. Experimental

2.1 Substrate preparation

ITO coat glass substrates were cleaned by sequential ultrasonic treatment in a detergent, deionized water, and isopropyl alcohol (IPA) for 30 min.

2.2 Sample preparation

PbI₂ precursor (1.1M, TCI 99.99%) was dissolved in N,N-dimethylformamide (DMF, Wako) and stirred at 70°C for at least 2 h to allow completed dissolution of solute. CH₃NH₃I (MAI, Wako) solution was mixed with 2-propanol (IPA, Wako) in various concentrations (0.038M, 0.05M, and 0.063M). A spiro-OMeTAD solution was prepared by dissolving spiro-OMeTAD (73 mg, Wako) in chlorobenzene (1 ml, Sigma-Aldrich 99.8%). Afterwards, 4-tert-butyl pyridine (28.8 μl, Sigma-Aldrich) and lithium bis(trifluoromethanesulfonyl)imide (Li-TFSI) solution (17.5 μl, 520 mg Li-TFSI in 1 ml acetonitrile, Sigma-Aldrich, 99.8%) were added.

2.3 TiO₂ compact layer preparation

TiO₂ solution was prepared by mixing TiC₁₆H₂₈O₆ (2.5 ml, Sigma-Aldrich, 99.8%) and ethanol (17.5 ml). ITO substrate was slowly heated on a hot plate from room temperature to 420°C. TiO₂ solution was sprayed on ITO substrates in every 10 sec for 10 min. After spray pyrolysis, temperature was increased to 450°C for 30 min.

2.4 Device fabrication

CH₃NH₃PbI₃ (1.1M) was formed using two-step deposition method. PbI₂ was spin-coated on the compact TiO₂ film at 3,000 rpm for 2 s and 6,000 rpm for 30 s (without loading time). The film was dried at 100°C for 60 min and then cooled to room temperature. The PbI₂-coated substrate was dipped into MAI solution (0.038M, 0.05M, and 0.063M) with different times (3, 5, and 10 min) and then heated at 110°C for 60 min. A spiro-OMeTAD solution was spin-coated on the CH₃NH₃PbI₃ perovskite layer at 4,000 rpm for 30 s. Finally, a gold (Au) electrode was thermally evaporated onto spiro-OMeTAD film to complete the devices. It should be noted that the base conditions of each experiment were performed as follows: (1) for effect of MAI concentration (set A), the MAI concentration was changed, while the duration time of MAI dipping time and the perovskite annealing time were 3 min and 60 min, respectively; (2) for effect of duration time in MAI dipping (set B), the MAI dipping time was changed, while the MAI concentration was the best condition from set A (the perovskite annealing time was 60 min); and (3) for effect of perovskite annealing time (set C), the perovskite annealing time was changed, while other conditions were the best ones observed from sets A and B experiments.

2.5 Sample characterizations

Photocurrent density-voltage (*J-V*) curves were measured under ambient atmosphere and simulated solar light, AM 1.5, 100 mW/cm², using a solar simulator with a xenon lamp. The light intensity of illumination source was calibrated using a standard 2.5×2.5 cm² silicon reference cell. The active area of the device was defined with a metal aperture mask of approximately 0.5×1 cm². Field emission scanning electron microscopy (FE-SEM) was used to investigate the morphology of perovskite layers.

3. Results and discussion

An inverted hybrid perovskite solar cell was fabricated in a configuration of ITO/compact TiO₂ (electron transporting layer)/perovskite (active layer)/Spiro-OMeTAD (hole transporting layer)/Au as shown in Figure 1. This device architecture is compatible with mass production process, because its lower temperature process (450°C) than Si-based solar cell (>1000°C). Spray pyrolysis in the compact TiO₂ layer has also potential to support mass production process. Moreover, this device architecture is easy to make further a tandem cell structure, because of its appropriated energy-band diagram (Figure 2).

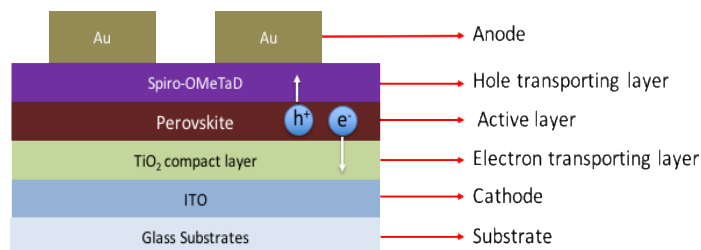


Figure 1. Structure of inverted perovskite solar cell (ITO/compact TiO₂/perovskite/Spiro-OMeTAD/Au).

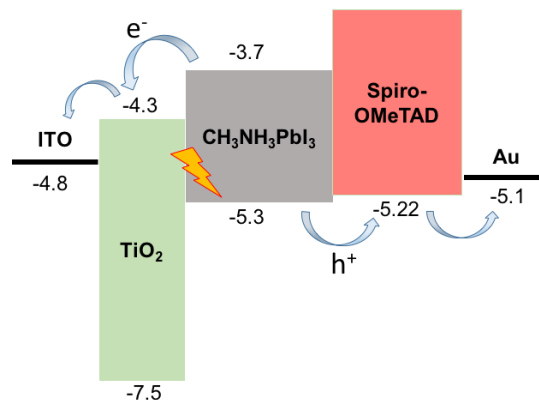


Figure 2. Energy band diagram of the inverted perovskite solar cell with a configuration of ITO/compact TiO₂/perovskite/Spiro-OMeTAD/Au.

3.1 Effect of MAI concentration

Generally, perovskite layer in perovskite solar cells was formed from the reaction of PbI₂ and MAI [13]. In order to achieve efficient perovskite morphology, the optimum MAI concentration was firstly studied in this work. SEM images in Figure 3 illustrate different crystal sizes of perovskite with different MAI concentration. The lower MAI concentration (0.038 M), the bigger crystal forms, due to its less nucleation and high growth of perovskite, as shown in Figures 3a-c. Therefore, at low MAI concentration, the surface of substrates showed low perovskite structure coverage. At the highest MAI concentration (0.063 M), the crystals provided the smallest cuboid perovskite size (diameter ~200 nm, Figure 3g-i) because nucleation and growth are already terminated at the initial stage [14]. It was reported that the MAPbI₃ size is significantly influenced on photovoltaic performance.

Figure 4 shows photocurrent density-voltage (*J-V*) curves of inverted perovskite devices with different CH₃NH₃I concentrations, while the photovoltaic parameters are concluded in Table 1. Figure 4 and Table 1 demonstrate that the power conversion efficiency is strongly influenced by MAI concentration. At lower MAI concentration (0.038 M), it showed high *J_{sc}* due to light scattering by the large-sized perovskite cuboids. However, the surface of substrate provided low perovskite structure coverage, thus it made *V_{oc}* low and obtained poor PCE. At the highest MAI concentration (0.063 M), it demonstrated the lowest *J_{sc}* because of much existing small-sized perovskite cuboids, resulting in increasing grain boundaries. It affected adversely charge recombination. At the medium MAI concentration (0.050 M), it can achieve the best PCE of 3.76% with outstanding *J_{sc}* (13.77 mAcm⁻²), *V_{oc}* (0.72 V), and FF (0.38), since it could be smoother and more uniform perovskite films than others. This results agreed with a report of Im et al. [14]. Therefore, suitable MAI concentration for fabrication of

inverted perovskite solar cells is not too low or too high. The balance between uniformity on the surface and small size of perovskite cuboids should be considered.

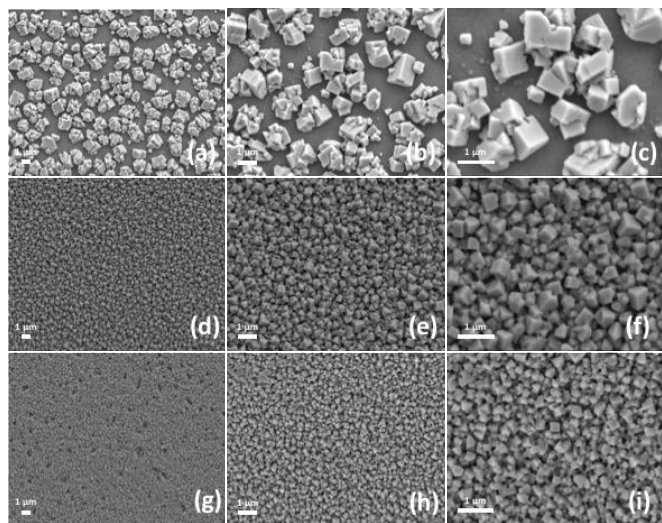


Figure 3. SEM images of perovskite crystals at different $\text{CH}_3\text{NH}_3\text{I}$ concentrations (a-c) 0.038 M, (d-f) 0.050 M, and (g-i) 0.063 M (scale bars in all images are 1 μm).

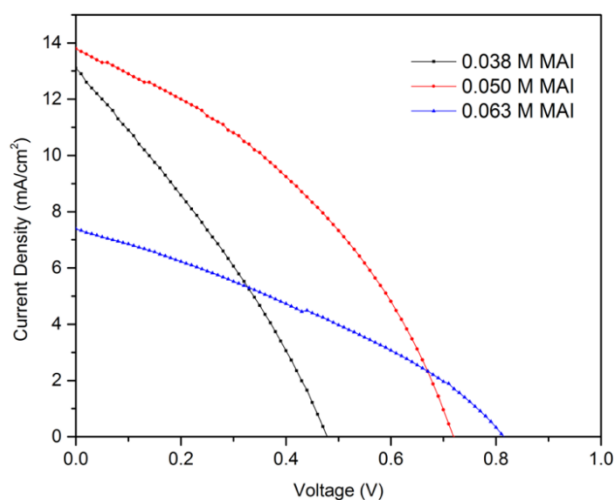


Figure 4. Photocurrent density-voltage (J - V) curves of inverted perovskite devices with different $\text{CH}_3\text{NH}_3\text{I}$ concentrations.

3.2 Effect of duration time in MAI dipping

One of the main parameters controlling perovskite morphology and photovoltaic performance of perovskite solar cell via 2-step deposition method is the duration time in MAI dipping. The effect of MAI dipping duration time on film morphology was elucidated via SEM images (Figure 5a-i). They showed some big pores and not smooth film via MAI dipping time for only 3 min, because of less loading time of the reaction. It might be that PbI_2 could not completely transform to perovskite (MAPbI_3) cuboids. In the other words, it has some leftover PbI_2 . Therefore, its poor morphology showed the effect on photovoltaic parameters (i.e. low J_{sc} of 11.67 mA/cm^2 , low V_{oc} of 0.73 V, low FF of 0.31, and low PCE of 2.62%), as shown in Figure 6 and Table 2. At 5 min of

MAI dipping time, increasing time could improve the transformation of PbI_2 to pure perovskite crystals [15]. Moreover, it demonstrated a smoother film, less porous surface, and homogeneous crystal size, as shown in Figure 5d-f. Besides, the best performance of device was achieved (PCE of 3.73% with the highest J_{sc} of 14.82%, and high V_{oc} and FF of 0.77 and 0.33, respectively). However, if the prolonging reaction time (MAI dipping duration time) overabundantly increased, the defects on surface would occur (voids and pinholes). The increasing amounts of defect influenced the charge recombination and photovoltaic parameters. Accordingly, the performance of device via MAI dipping time of 10 min presented on lower J_{sc} and lower efficiency, compared with the performance of device via MAI dipping time of 5 min. Hence, the MAI dipping time of 5 min is appropriate for the inverted perovskite solar cell fabrication.

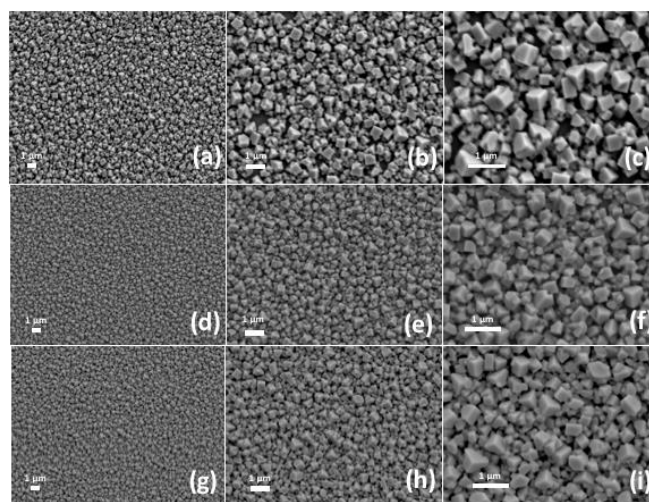


Figure 5. SEM images of perovskite crystals at different $\text{CH}_3\text{NH}_3\text{I}$ dipping duration times (a-c) 3 min, (d-f) 5 min, and (g-i) 10 min (scale bars in all images are 1 μm).

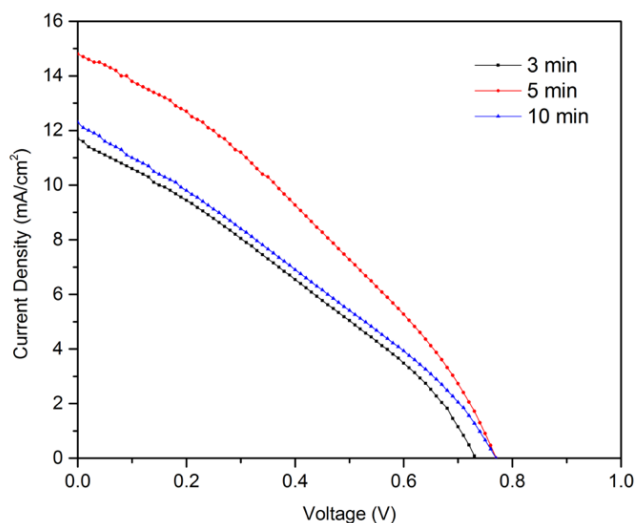


Figure 6. Photocurrent density-voltage (J - V) curves of inverted perovskite devices with different $\text{CH}_3\text{NH}_3\text{I}$ dipping duration times.

Table 1. Performances and photovoltaic characteristics of inverted perovskite solar cells with different CH₃NH₃I concentrations.

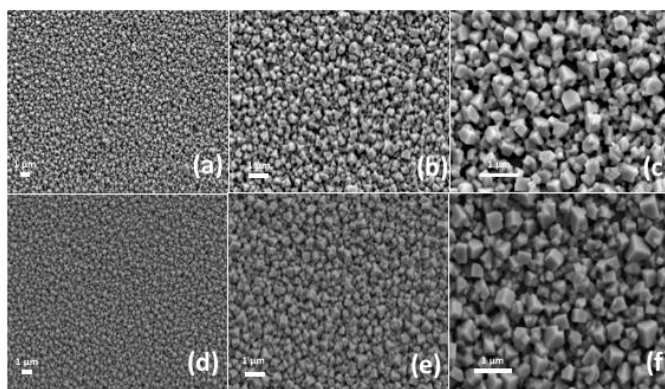
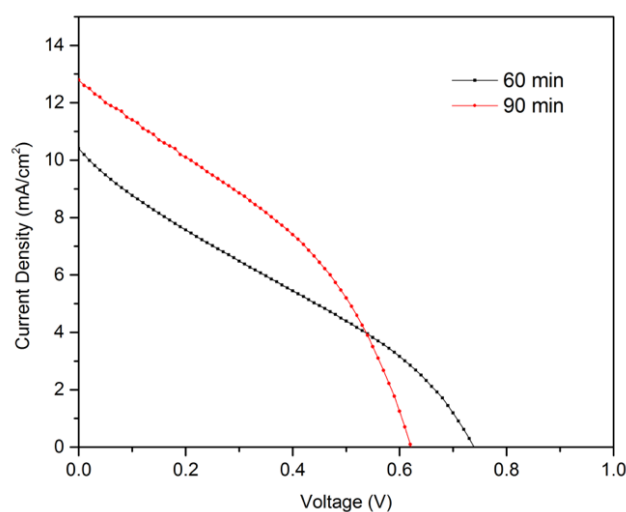
Device	MAI concentration	J_{sc} (mA/cm ²)	V_{oc} (V)	FF	PCE (%)
1	0.038 M	13.09	0.48	0.30	1.85
2	0.050 M	13.77	0.72	0.38	3.76
3	0.063 M	7.38	0.82	0.33	1.99

Table 2. Performances and photovoltaic characteristics of inverted perovskite solar cells with different CH₃NH₃I dipping times.

Device	MAI dipping time (min)	J_{sc} (mA/cm ²)	V_{oc} (V)	FF	PCE (%)
1	3	11.67	0.73	0.31	2.62
2	5	14.82	0.77	0.33	3.73
3	10	11.83	0.77	0.33	3.02

Table 3. Performances and photovoltaic characteristics of inverted perovskite with different perovskite annealing times.

Device	Perovskite annealing time (min)	J_{sc} (mA/cm ²)	V_{oc} (V)	FF	PCE (%)
1	60	10.39	0.74	0.29	2.22
2	90	12.75	0.62	0.37	2.97

**Figure 7.** SEM images of perovskite crystals at different perovskite annealing times (a-c) 60 min, (d-f) 90 min (scale bars in all images are 1 μm).**Figure 8.** Photocurrent density-voltage (J - V) curves of inverted perovskite devices with different perovskite annealing times.

3.3 Effect of perovskite annealing time

The perovskite annealing time changed the film morphology, resulting in different photovoltaic performances. Perovskite layers should be annealed for at least 1 h. At annealing of perovskite with only 60 min, the surface indicated some big pores and non smooth films, as shown in Figure 7a-c. Therefore, the PCE just obtained only 2.22% with poor photovoltaic parameters, as shown in Figure 8 and Table 3. At the perovskite annealing time of 90 min, the higher performance can achieve with PCE of 2.97% (with higher J_{sc} and FF of 12.75 mAcm⁻² and 0.37, respectively), because when thermal annealing time increased, the grain of perovskite crystal size increased, hence minimization of grain boundary and allowed more inter-diffusion [16]. Nevertheless, if the perovskite film was annealed for longer time, it might be defect in perovskite crystals and it could decompose the perovskite films.

4. Conclusion

Inverted hybrid perovskite devices with a structure of ITO/compact TiO₂/perovskite/Spiro-OMeTAD/Au were fabricated and studied. Effects of three conditions (*i.e.* (1) MAI concentrations, (2) MAI dipping duration times, and (3) perovskite annealing times) on obtained morphology and photovoltaic performance in inverted perovskite solar cells with a compact TiO₂ layer (fabricated by spray pyrolysis) were investigated. The optimized morphologies and performances can be obtained from 0.05 M MAI concentration, 5 min MAI dipping duration time, and 90 min perovskite annealing time.

Acknowledgements

The authors would like to acknowledge Center of Excellence on Energy Technology and Environment and The Joint Graduate School of Energy and Environment (JGSEE) for academic and financially supports. The authors also thank the Academic Cooperation Agreement Program (ACAP) of Tokyo Institute of Technology for supporting experiments.

References

- [1] Cui J, Yuan H, Li J, Xu X, Shen Y, Lin H, Wang M, Recent progress in efficient hybrid lead halide perovskite solar cells, *Science and Technology of Advanced Materials* 16/3 (2015).
- [2] Fan J, Jia B, Gu M, Perovskite-based low-cost and high-efficiency hybrid halide solar cells, *Photonics Research* 2/5 (2014) 111.
- [3] Boroumandnia A, Kasaeian AB, Nikfarjam AR, Mohammadpour R, Effect of TiO₂ nanofiber density on organic-inorganic based hybrid solar cells (RESEARCH NOTE), *International Journal of Engineering* 27/7(A) (2014) 1133-1138.
- [4] Wang D, Wright M, Elumalai NK, Uddin A, Stability of perovskite solar cells. *Solar Energy Materials and Solar Cells* 147 (2016) 255-275.
- [5] Jeon T, Geffroy B, Tondelier D, Yu L, Jegou P, Jusselme B, Palacin S, Roca i Cabarrocas P, Bonnassieux Y, Effects of acid-treated silicon nanowires on hybrid solar cells performance, *Solar Energy Materials and Solar Cells* 117 (2013) 632-637.
- [6] Zhou H, Chen Q, Li G, Luo S, Song T-b, Duan H-S, Hong Z, You J, Liu Y, Yang Y, Interface engineering of highly efficient perovskite solar cells, *Science* 345/6196 (2014) 542-546.
- [7] Liu M, Johnston MB, Snaith HJ, Efficient planar heterojunction perovskite solar cells by vapour deposition, *Nature* 501/7467 (2013) 395-398.
- [8] Luo D, Yu L, Wang H, Zou T, Luo L, Liu Z, Lu Z, Cubic structure of the mixed halide perovskite CH₃NH₃PbI_{3-x}Cl_x via thermal annealing, *RSC Adv* 5/104 (2015) 85480-85485.
- [9] Susrutha B, Giribabu L, Singh SP, Recent advances in flexible perovskite solar cells., *Chem Commun* 51/79 (2015) 14696-14707.
- [10] Burschka J, Pellet N, Moon S-J, Humphry-Baker R, Gao P, Nazeeruddin MK, Grätzel M, Sequential deposition as a route to high-performance perovskite-sensitized solar cells., *Nature* 499/7458 (2013) 316-319.
- [11] Eze VO, Lei B, Mori T, Air-assisted flow and two-step spin-coating for highly efficient CH₃NH₃PbI₃ perovskite solar cells, *Japanese Journal of Applied Physics* 55/2 (2016).
- [12] Lee J-W, Park N-G, Two-step deposition method for high-efficiency perovskite solar cells, *MRS Bulletin* 40/8 (2015) 654-659.
- [13] Zhang WH, Cai B, Organolead halide perovskites: A family of promising semiconductor materials for solar cells, *Chinese Science Bulletin* 59/18 (2014) 2092-2101.
- [14] Im J-H, Jang I-H, Pellet N, Grätzel M, Park N-G, Growth of CH₃NH₃PbI₃ cuboids with controlled size for high-efficiency perovskite solar cells, *Nature Nanotechnology* 9/11 (2014) 927-932.
- [15] Zhao JJ, Wang P, Liu ZH, Wei LY, Yang Z, Chen HR, Fang XQ, Liu XL, Mai YH, Controlled reaction for improved CH₃NH₃PbI₃ transition in perovskite solar cells, *Dalton Trans* 44/40 (2015) 17841-17849.
- [16] Barnett JL, Cherrett, VL, Hutcherson CJ, So MC, Effects of solution-based fabrication conditions on morphology of lead halide perovskite thin film solar cells, *Advances in Materials Science and Engineering* 2016 (2016).